

Article

Assessing Golden Tides from Space: Meteorological Drivers in the Accumulation of the Invasive Algae *Rugulopteryx okamurae* on Coasts

Sara Haro ^{1,2} , Liam Morrison ², Isabel Caballero ³ , Félix L. Figueroa ¹ , Nathalie Korbee ¹ , Gabriel Navarro ³  and Ricardo Bermejo ^{1,*}

¹ Departamento de Ecología y Geología, Facultad de Ciencias, Instituto Andaluz de Biotecnología y Desarrollo Azul, Universidad de Málaga, 29010 Malaga, Spain; sara.haro@uma.es (S.H.); felixfigueroa@uma.es (F.L.F.); nkorbee@uma.es (N.K.)

² Earth and Life Sciences, School of Natural Sciences and Ryan Institute, University of Galway, H91 TK33 Galway, Ireland; liam.morrison@universityofgalway.ie

³ Departamento de Ecología y Gestión Costera, Instituto de Ciencias Marinas de Andalucía (ICMAN), Consejo Superior de Investigaciones Científicas (CSIC), 11510 Cadiz, Spain; isabel.caballero@icman.csic.es (I.C.); gabriel.navarro@icman.csic.es (G.N.)

* Correspondence: ricardo.bermejo@uma.es

Abstract: Massive accumulations of invasive brown algae *Rugulopteryx okamurae* are exacerbating environmental and socio-economic issues on the Mediterranean and potentially Atlantic coasts. These golden tides, likely intensified by global change processes such as changes in wind direction and intensity and rising temperatures, pose increasing challenges to coastal management. This study employs the Normalized Difference Vegetation Index (NDVI), with values above 0.08 from Level-2 Sentinel-2 imagery, to effectively monitor these strandings along the coastline of Los Lances beach (Tarifa, Spain) in the Strait of Gibraltar Natural Park from 2018 to 2022. Los Lances beach is one of the most affected by the *R. okamurae* bioinvasion in Spain. The analysis reveals that wind direction determines the spatial distribution of biomass accumulated on the shore. The highest average NDVI values in the western patch were observed with south-easterly winds, while in the eastern patch, higher average NDVI values were recorded with south-westerly, westerly and north-westerly winds. The maximum coverage correlates with elevated temperatures and minimal rainfall, peaking between July and October. Leveraging these insights, we propose a replicable methodology for the early detection and strategic pre-shore collection of biomass, which could facilitate efficient coastal cleanup strategies and enhance biomass utility for biotechnological applications. This approach promises cost-effective adaptability across different geographic areas impacted by golden tides.



Citation: Haro, S.; Morrison, L.; Caballero, I.; Figueroa, F.L.; Korbee, N.; Navarro, G.; Bermejo, R. Assessing Golden Tides from Space: Meteorological Drivers in the Accumulation of the Invasive Algae *Rugulopteryx okamurae* on Coasts. *Remote Sens.* **2024**, *16*, 2689.

<https://doi.org/10.3390/rs16152689>

Academic Editor: John Dymond

Received: 19 June 2024

Revised: 19 July 2024

Accepted: 20 July 2024

Published: 23 July 2024



Copyright: © 2024 by the authors. Licensee MDPI, Basel, Switzerland. This article is an open access article distributed under the terms and conditions of the Creative Commons Attribution (CC BY) license (<https://creativecommons.org/licenses/by/4.0/>).

1. Introduction

The enormous accumulation of fast-growing brown macroalgae, often referred to as “golden tides”, poses significant environmental and socio-economic challenges along coastlines worldwide. These challenges include the unsightly mass of algal decay on coastlines, disruption of local ecosystems, anoxic events, unpleasant odours, and negative impacts on tourism and management costs [1]. Examples include *Sargassum* spp. on the Chinese and Caribbean coasts [2], *Ectocarpus siliculosus* along the eastern coast of Ireland [3,4], *Lobophora variegata* in the Macaronesia islands [5], and *Rugulopteryx okamurae* on the western Mediterranean coast [6]. The massive blooms of seaweeds, both native and invasive, generate disruptive events altering the functioning of marine ecosystems. These alterations result in the competitive exclusion of other species, the physical obliteration of other habitat-forming species, changes in trophic networks, dystrophic events, and other

processes, reducing the value of ecosystem services, including nutrient cycling and climate resilience, as well as the economic impact of beach-cast algae on sectors such as tourism and recreational activities [1,7]. The causes and mechanisms underlying the occurrence of macroalgal blooms are diverse and multifactorial [8]. Factors such as eutrophication [9], alterations in oceanic currents [1], and the introduction of alien species (e.g., [10,11]) are commonly recognized as primary triggers for these events.

Biological invasions are one of the most pervasive forms of pollution, and their effects are often irreversible. There is a general consensus in the scientific community about the impossibility of eradicating marine invasive seaweeds once they become established [12,13]. To date, attempts to eradicate widely distributed alien seaweeds have failed, including multimillion-dollar programmes to remove *Undaria pinnatifida* from Tasmania and New Zealand and *Sargassum muticum* from the UK [14,15]. The only reported successful experience was the eradication of *Caulerpa taxifolia* in California, which was accomplished at the initial stages of infestation at a cost of USD 7 million [16]. Considering the impossibility of eradicating well-established invasive seaweeds in marine environments, environmental management strategies might focus on the prevention and detection of the arrival of alien species and on reducing or minimizing the negative impact to an acceptable level once the species becomes established [12].

Rugulopteryx okamurae [17] (Dictyotales, Phaeophyceae), a brown seaweed originally from the northeastern Pacific Ocean, was first reported in the Mediterranean Sea on the French coast (Thau lagoon) in spring 2002, likely introduced with Japanese oysters for aquaculture [18,19]. However, *R. okamurae* did not become invasive in new territories until autumn 2015, when this species produced large golden tides that affected the coasts of the Strait of Gibraltar [20,21]. This alien seaweed has spread rapidly due to its reproductive characteristics, survival, regrowth capacity, and favourable environmental conditions [22]. Since 2015, this species has been observed spreading along the western Mediterranean Sea and Macaronesia, with records documenting its presence on the northeast Atlantic Islands of Portugal (mainly in the Azores and Madeira) [23], the Andalusian coast (mainly the Strait of Gibraltar and the Alboran Sea) and the Levante coast (specifically, Alicante) in Spain [6,24], the northwest of Morocco [25], and the northwest Mediterranean coast of France (Marseille region) [19], and it has even reached Italy along the northwestern coast of Sicily [26].

R. okamurae forms dense mats on rocky substrates in subtidal zones that drift towards shorelines. In addition to rocky bottoms, this species also grows epiphytically on coral-ligenous organisms, cold-water corals, and artificial substrates, colonizing a wide range of habitats from 0 to 40 m depth [6,27]. Increases in water temperature and nutrients (mainly nitrate and phosphate) in the upper layers (up to 30 m) in recent years are thought to contribute to this bioinvasion [6,28]. This dominance alters marine ecosystems by displacing native habitat-forming species (mainly, seagrass meadows or coralline seaweeds), leading to decreased biodiversity and diminishing the quantity and quality of ecosystem services (e.g., negatively impacting fisheries, or tourism as a consequence of the accumulation of these golden seaweed tides along the coastline) [6,29–32].

In order to allow the recreational use of beaches in the area of the Strait of Gibraltar and other affected areas, local authorities are removing large quantities of this seaweed washed ashore, which incurs significant economic costs [33]. For instance, the town councils of Spanish beaches affected by *R. okamurae* strandings, located within and around the Natural Park of the Strait of Gibraltar, reported a minimum cost of EUR 730,000 from 2020 to 2023. Specifically, during the summer of 2021, the town of Tarifa (located on the Andalusian coast in southern Spain) reported removing 6213 tons of *R. okamurae* biomass that had accumulated on the shore, at a cost of EUR 63,275.75 [34]. Overall, bloom biomass (regardless of the seaweed species) is piled along the shoreline to be later removed mechanically and deposited in landfills, which results in increased management costs [35,36]. Exploring alternative uses for this biomass could offset these costs. Biotechnological valorization of beach-cast algae, including exotic species, has been reported as a management

strategy for residual biomass, contributing to the reduction of costs associated with beach collection [5,37–39]. However, the presence of chemical compounds of concern to human health [35,40,41] and large amounts of sand can compromise the quality of the biomass and its utilization. Moreover, the mechanical removal of algal biomass from the shore often leads to significant sand loss. The removal process not only extracts the biomass but also sand and bioclasts trapped within it, resulting in an estimated 10% of the total volume removed consisting of sand [42]. This issue may be especially relevant in areas affected by coastal erosion.

Based on all the above, it is crucial to investigate the factors that increase the accumulation of *R. okamurae* strandings along the coastline. Large brown algal strandings were associated with specific wind conditions that facilitated the transportation and deposition of this seaweed on beaches, or occurred more frequently during warm months [4,43,44]. Moreover, phenomena such as windstorms and elevated temperatures, associated with global change processes, could be facilitating the arrival of invasive species [45]. Hence, understanding the role that meteorological factors play in the spatiotemporal dynamics of *R. okamurae* strands along the coastline is essential for developing effective management strategies to mitigate its negative impacts on the service sector as well as to establish protocols that allow for its collection before it reaches the shore. These strategies aim to minimize the costs of removal from beaches, reduce the loss of beach sand associated with cleaning operations, and to favour the collection of higher quality fresh *R. okamurae* biomass. This is particularly important given that *R. okamurae* biomass can be potentially used in the production of biogas, composting, bioplastics, biomaterials, and cosmetic and pharmaceutical applications, as well as in the creation of other value-added products [46,47].

For monitoring *R. okamurae* distribution along the coastline, Sentinel-2 satellite imagery offers a critical resource for developing cost-effective management tools with its 10 m spatial resolution and a high revisit frequency of 5 days at the Equator. Earth Observation (EO) technologies have been instrumental in tracking the golden seaweeds, combining field sampling with satellite data [4,48,49], machine learning [50], deep learning [51,52], and other artificial intelligence algorithms [53]. EO technologies to map *R. okamurae* both washed ashore and floating on the water surface across intertidal zones were utilized, employing a Support Vector Machine algorithm in combination with unmanned aerial vehicles and satellite imagery from Sentinel-2 and Landsat-8 at Bolonia Beach on the Andalusian coast of Spain [54]. This approach, however, might encounter challenges when replicated in different locations or times due to the “black-box” nature of machine learning models [55]. A comparable methodology for identifying golden tides, using NDVI values derived from Sentinel-2 imagery to map *R. okamurae* distribution at Bolonia Beach, has also been validated (see Supplementary Material of [4]). Their findings showed that NDVI values above 0.08 are effective in monitoring the spatiotemporal dynamics of golden seaweed biomass along shorelines, enhancing its replicability over space and time. To date, these two studies represent the only instances where EO technologies have been utilized to monitor the dead biomass of *R. okamurae*.

Therefore, the primary objective of this study was to map the extent of the invasive brown seaweed, *Rugulopteryx okamurae*, along the Andalusian coastline, focusing specifically on Los Lances beach in Tarifa, located within the Strait of Gibraltar Natural Park. The choice of Los Lances beach as the case study is justified due to its significant impact from *R. okamurae* strandings, making it one of the most affected beaches (Figure S1) [6,34]. Sentinel-2 satellite imagery was used to assess for the first time the spatiotemporal distribution of *R. okamurae* along the shore over a five-year period (2018–2022), and to analyse its relationship with meteorological factors. This research aims to develop a comprehensive understanding that could facilitate the generation of a protocol for the preventive collection of *R. okamurae* biomass before it reaches the shore. Such a protocol would leverage its potential for biotechnological applications and mitigate negative impacts on tourism and benthic communities along the coastline, as well as reduce the costs associated with keeping

the coasts clean [33,46,56]. The potential of this study lies in its applicability to other areas affected by seaweed tides.

2. Materials and Methods

2.1. Study Site

The present study focuses on Los Lances beach located in Tarifa, Andalusia, Southern Spain. Los Lances is a sandy beach ($36^{\circ}02'24''\text{N}$, $5^{\circ}38'04''\text{W}$) situated within the Strait of Gibraltar Natural Park (Figure 1). The *Playa de Los Lances* Natural Area covers 226 hectares to the west of the town centre [33]. The area of interest was manually delimited from satellite imagery acquired during the lowest tide, covering 57.68 ha and a length of 6.5 km (Figure 1).

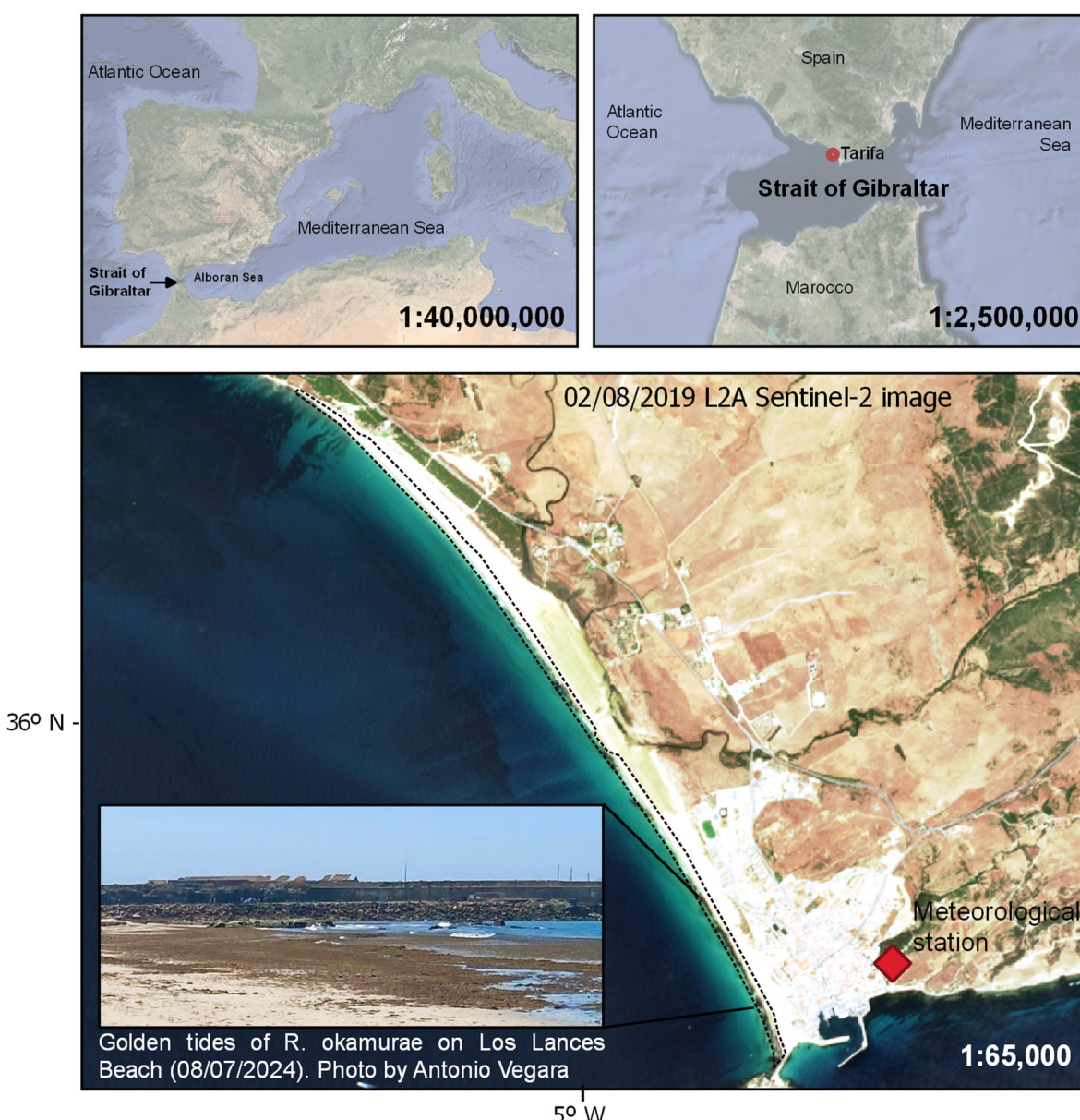


Figure 1. Location of Los Lances Beach (Tarifa, Cadiz, SW Spain) in the Natural Park of the Strait of Gibraltar, one of the areas most affected by *R. okamurae* strandings. The study area, i.e., the coastline, is marked with a discontinuous black line. The Level 2 Sentinel-2 True Color image, acquired on 2 August 2019, shows the strandings at the eastern ends of the beach. A photo of *R. okamurae* strandings in that area is also included. The meteorological station is indicated with a red rhombus.

2.2. Sentinel-2 Data Processing

Sentinel-2 multispectral satellite images, cloud-free, and obtained at low tide, were manually selected from the Sentinel Hub EO Browser (Figure 2; step 1). A total of 130 Sentinel-2 images (Level 2A) from 2018 to 2022 were processed using the Normalized Difference Vegetation Index (NDVI). NDVI was calculated using the red surface reflectance bands (sr_B4) and near-infrared (sr_B8) as follows: $NDVI = (sr_B8 - sr_B4) / (sr_B8 + sr_B4)$, where band 8 (B8) corresponds to reflectance at 850 nm and band 4 (B4) to reflectance at 650 nm. The NDVI is often used as a proxy of biomass to study intertidal photosynthetic communities (e.g., microphytobenthos, seagrass or seaweeds) during low tides [57–59]. Pixels with NDVI values above 0.08 were used to identify the presence of *R. okamurae* washed ashore (Figure 2; step 3). This approach follows the methodology for monitoring golden seaweed tides accumulated along the shoreline in the absence of other primary producers, which was validated for mapping *R. okamurae* in a nearby area (Figure S2) [4]. Google Earth Engine (GEE), a cloud-based geospatial analysis platform, facilitated the download of NDVI images filtered with values above 0.08 from 2018 to 2022. The “Sentinel-2 MSI: MultiSpectral Instrument, Level-2A” image collection (dataset availability from March 2017) was utilized for tile 29SQV, using a shapefile to define the area of interest (outlined with a discontinuous black line in Figure 1, and obtained through step 2 in Figure 2). All scenes were aligned in the WGS 84/UTM zone 29 N coordinate system (EPSG: 32629).

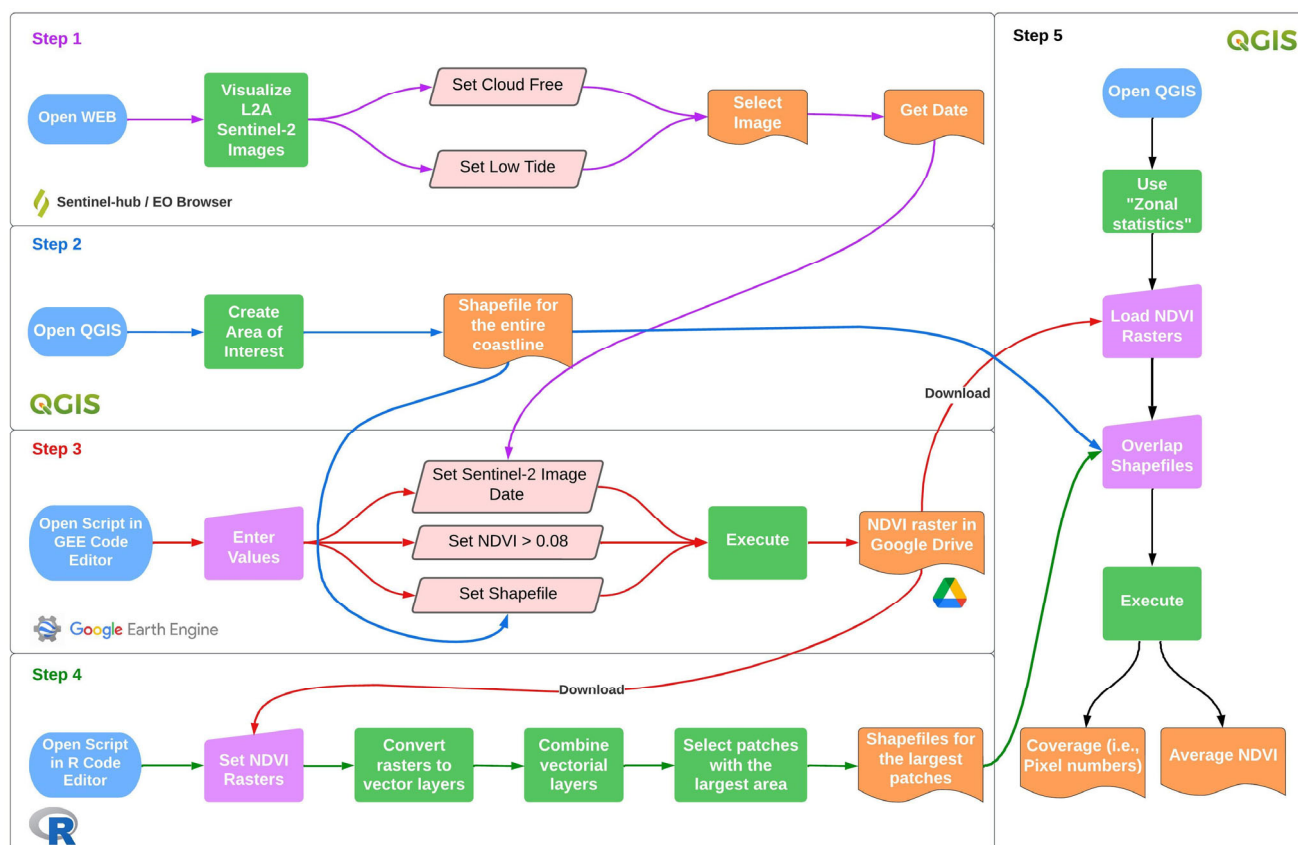


Figure 2. Flowchart showing the proposed methodology to monitor *R. okamurae* washed ashore. This comprises five steps: (step 1) visualization and selection of Sentinel-2 imagery to be processed; (step 2) creation of the area of interest, i.e., along the entire coastline; (step 3) processing of Sentinel-2 images using Google Earth Engine; (step 4) selection of the largest patches with seaweed accumulations; and (step 5) calculating coverage and average NDVI for the entire coastline and for the largest extension patches using geographic information system (GIS); where start (is plotted in blue), actions (in green), settings (in pink), inputs (in purple) and results (in orange).

2.3. Temporal and Spatial Dynamics

The *R. okamurae* coverage was determined based on the number of pixels with NDVI values above 0.08. Coverage and average NDVI of *R. okamurae* along the Los Lances beach coastline were calculated using the “Zonal statistics” plugin in QGIS software (version 3.10 A Coruña) (Figure 2; step 5). In addition to the area of interest (Los Lances beach coastline), two other vector layers were created to conduct the spatial analysis. To analyse the spatial variability and identify the area with maximum extensions of *R. okamurae*, the mean of all images or rasters (NDVI > 0.08) was calculated (Figure 3) using the “raster” and “sp” libraries in Rstudio (version 2022.07.2 + 576). All rasters were transformed into vector layers and combined among themselves to delimit the largest patches (Figure 2; step 4). Two patches were identified: the west patch (7 ha) and the east patch (16 ha) (Figure 3). The “dissolve” tool was applied to these vector layers to unify adjacent boundaries. This step was critical for calculating both the number of pixels indicating the presence of *R. okamurae* (i.e., coverage) and the average NDVI for the entire study area (i.e., along the entire coastline) as well as for the most extensive areas (i.e., each patch) (Figure 2; step 5).

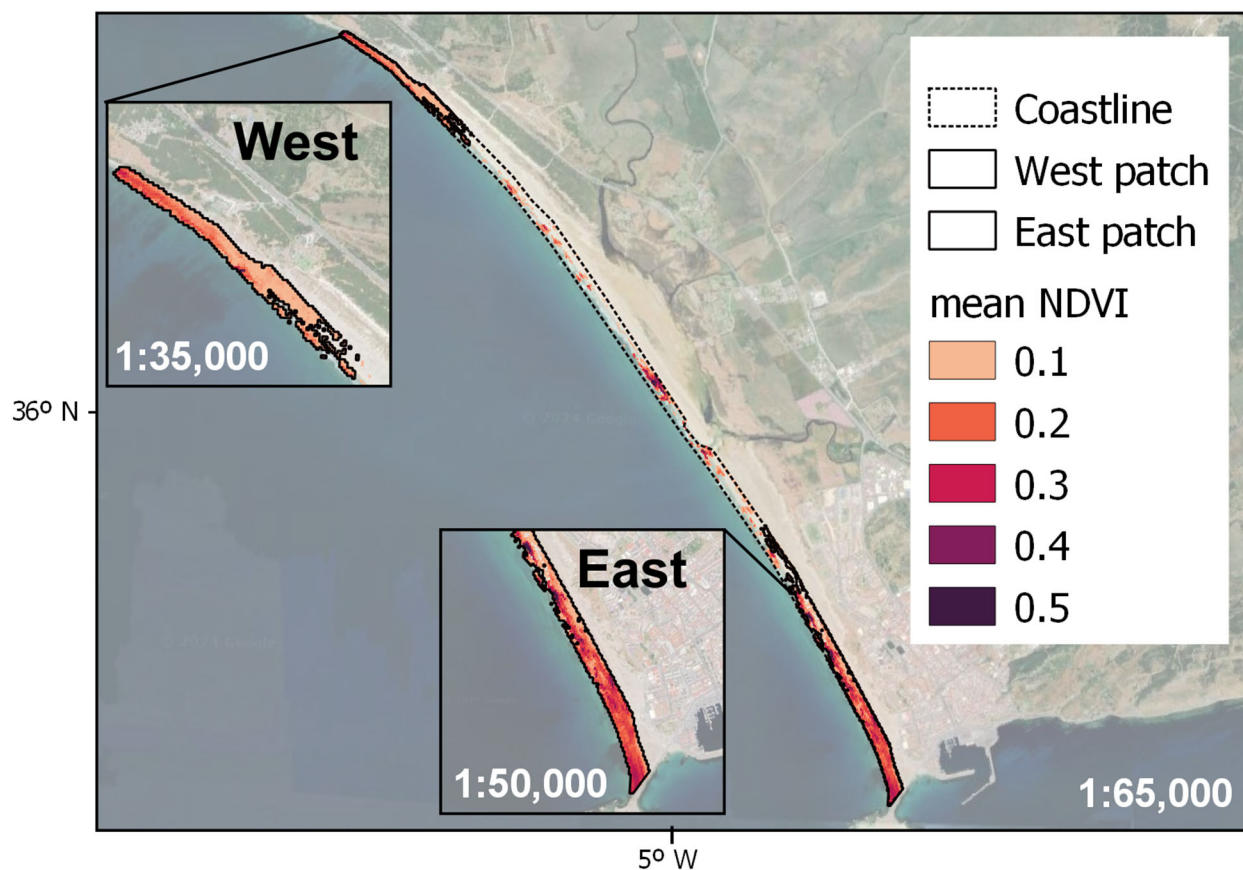


Figure 3. Average coverage and NDVI (NDVI > 0.08) for *R. okamurae* along Los Lances beach (Tarifa, Andalusia, Spain) from 130 Level-2 Sentinel-2 images (2018–2022). The coastline is marked with a discontinuous black line, with the maximum extension areas at the beach ends (east and west patches) indicated by a continuous black line.

2.4. Statistical Analysis

To evaluate the annual and monthly variability (temporal trends) of the coverage and the average NDVI of *R. okamurae* washed ashore, the Kruskal–Wallis statistical test was used after verifying that the data did not follow a normal distribution (Shapiro–Wilk test). These analyses were conducted using the software Rstudio (version 2022.07.2 + 576) and the “stats” package. Subsequently, the Spearman coefficient was calculated (using

the “Hmisc” and “corrplot” packages in R) between the coverage and the average NDVI (including, separately, the entire study area and the patches located at both ends of the beach) and the accumulated rainfall during the 5 days prior to the date the satellite captured the image. Averages of temperature, wind speed, and wind direction for the 5 days prior were also calculated. Averages for 3 and 7 days were also tested, with the highest Spearman coefficients observed for the 5-day period. Meteorological variables were obtained from the Tarifa weather station ($36^{\circ}01'08.3''\text{N}$; $5^{\circ}35'58.0''\text{W}$) located 1.3 km away in a direct line from the study area (Figure 1), and downloaded from the *Red de Información Ambiental de Andalucía* (REDIAM) of the *Junta de Andalucía*. In addition, Kruskal–Wallis statistical analysis was performed to elucidate the impact of wind direction on the coverage and average NDVI associated with *R. okamurae* strandings for the east and west patches. Following this, Dunn’s post hoc test with a Bonferroni correction was conducted to discern differences between individual groups using the “rstatix” and “stats” packages.

3. Results

3.1. Monitoring Spatiotemporal Dynamics

The average values between pixels with NDVI above 0.08 for all images analysed between 2018 and 2022 are presented in Figure 3. The average NDVI ranged from 0.08 to 0.68. An average coverage of 1.5 ha was estimated between 2018 and 2022, reaching a peak of 8 ha on 2 August 2019. The average coverage showed a significant monthly variability ($X^2 = 30.708$, $\text{df} = 11$, $p\text{-value} = 0.001$; Kruskal–Wallis) with peaks between July and October (Figure 4a). No interannual variability was observed for the coverage ($X^2 = 7.149$, $\text{df} = 4$, $p\text{-value} = 0.13$) (Figure 4b). For the average NDVI for the entire coastline, a seasonal pattern was not detected (Figure 4c); however, annual significant differences were identified between 2019 (0.21 ± 0.07 NDVI; mean \pm standard deviation) and 2022 (0.15 ± 0.06) ($p\text{-value} < 0.001$; Dunn’s post hoc test) (Figure 4d).

The highest *R. okamurae* accumulations were observed at the ends of the beach, eastern and western patches. Seasonal average maps of coverage and NDVI for both patches are shown in Figure 5, and their temporal variability (annual and monthly) was analysed (Figure 6). At the western end of the beach, patches of *R. okamurae* with an estimated size of up to 4 ha were recorded on 28 August 2020, and 6 ha at the eastern end on 2 August 2019. When analysing the temporal variability of the coverage and average NDVI for both patches separately, significant differences were only found between February and July for the eastern patch (Figure 6a,c), while annual differences were significant for both patches (Figure 6d). The average NDVI for the eastern patch showed significant differences between 2019 and 2020 ($p\text{-value} < 0.05$; Dunn’s post hoc test), and between 2019 and 2022 ($p\text{-value} < 0.001$). Similarly, the western patch showed differences between 2019 and 2020 and between 2020 and 2022, both with a $p\text{-value} < 0.001$.

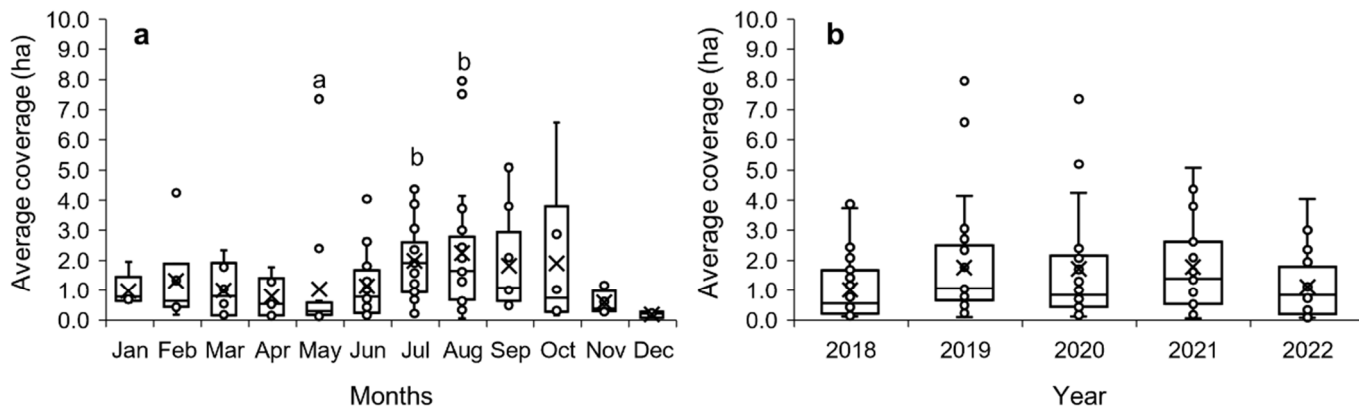


Figure 4. Cont.

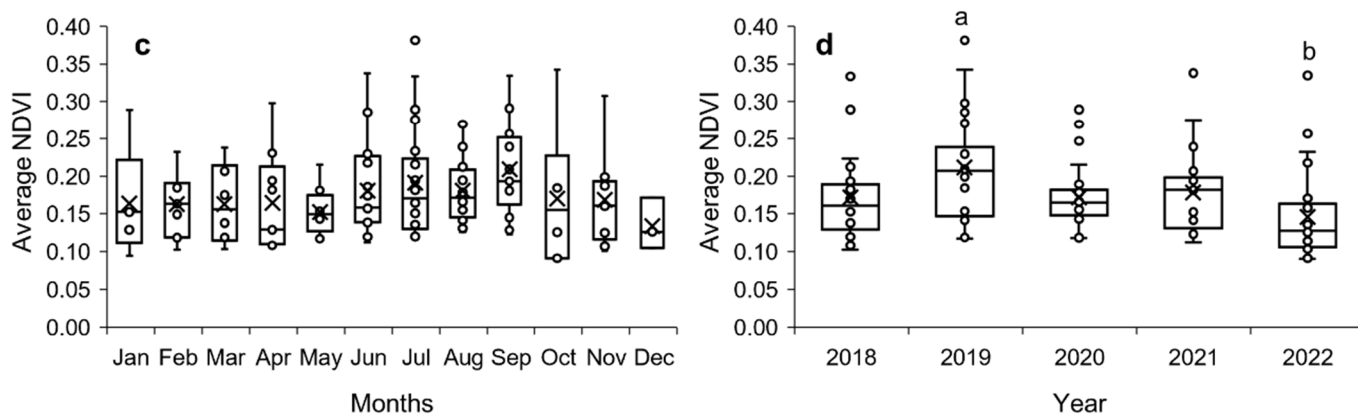


Figure 4. (a,b) Box plots depicting the average monthly and annual coverage of *R. okamurae* along the coastline from 2018 to 2022. (c,d) Box plots depicting the average monthly and annual NDVI (used as a proxy of *R. okamurae* biomass washed ashore) along the coastline from 2018 to 2022. The line within each box plot represents the median and the cross sign indicates the mean.

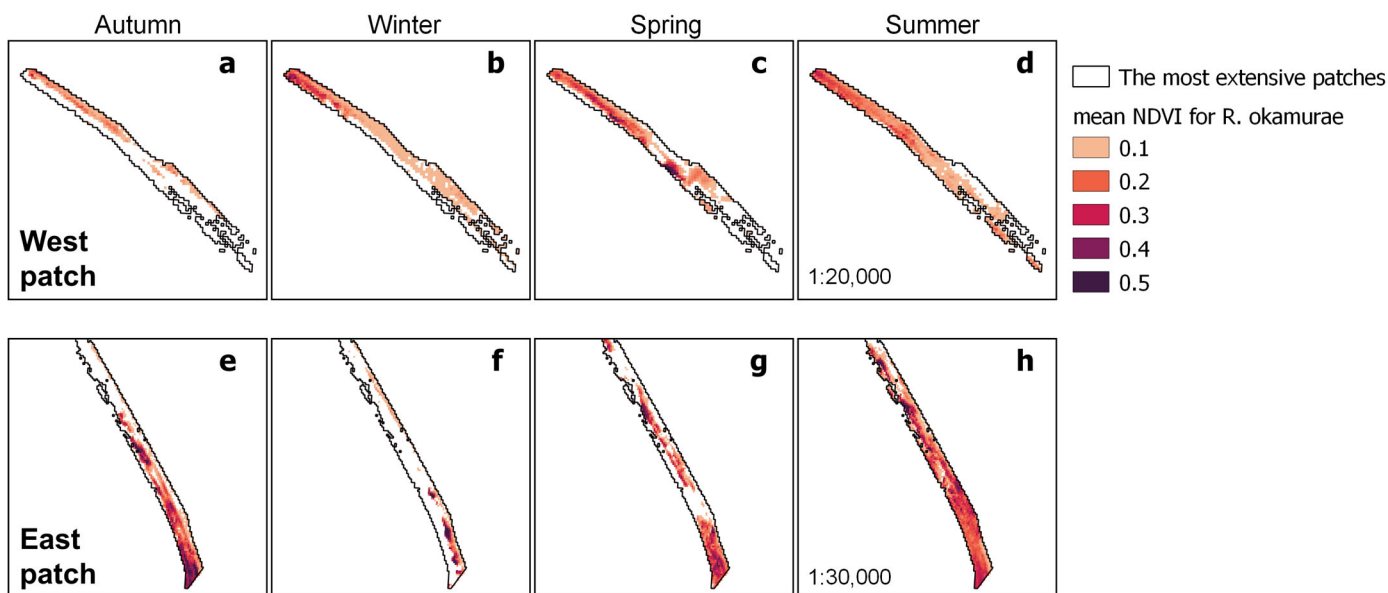


Figure 5. (a–d) Seasonal averages of coverage and NDVI associated with golden tides of invasive *R. okamurae* at the western end of Los Lances Beach (Tarifa, Andalusia, Spain). (e–h) Seasonal averages of coverage and NDVI associated with golden tides of invasive *R. okamurae* at the eastern end of Los Lances Beach (Tarifa, Andalusia, Spain). Averages were calculated using 22 autumn, 16 winter, 33 spring, and 59 summer Sentinel-2 images taken between 2018 and 2022. The seasons are defined as follows: autumn (21 September–21 December), winter (21 December–21 March), spring (21 March–21 June), and summer (21 June–21 September).

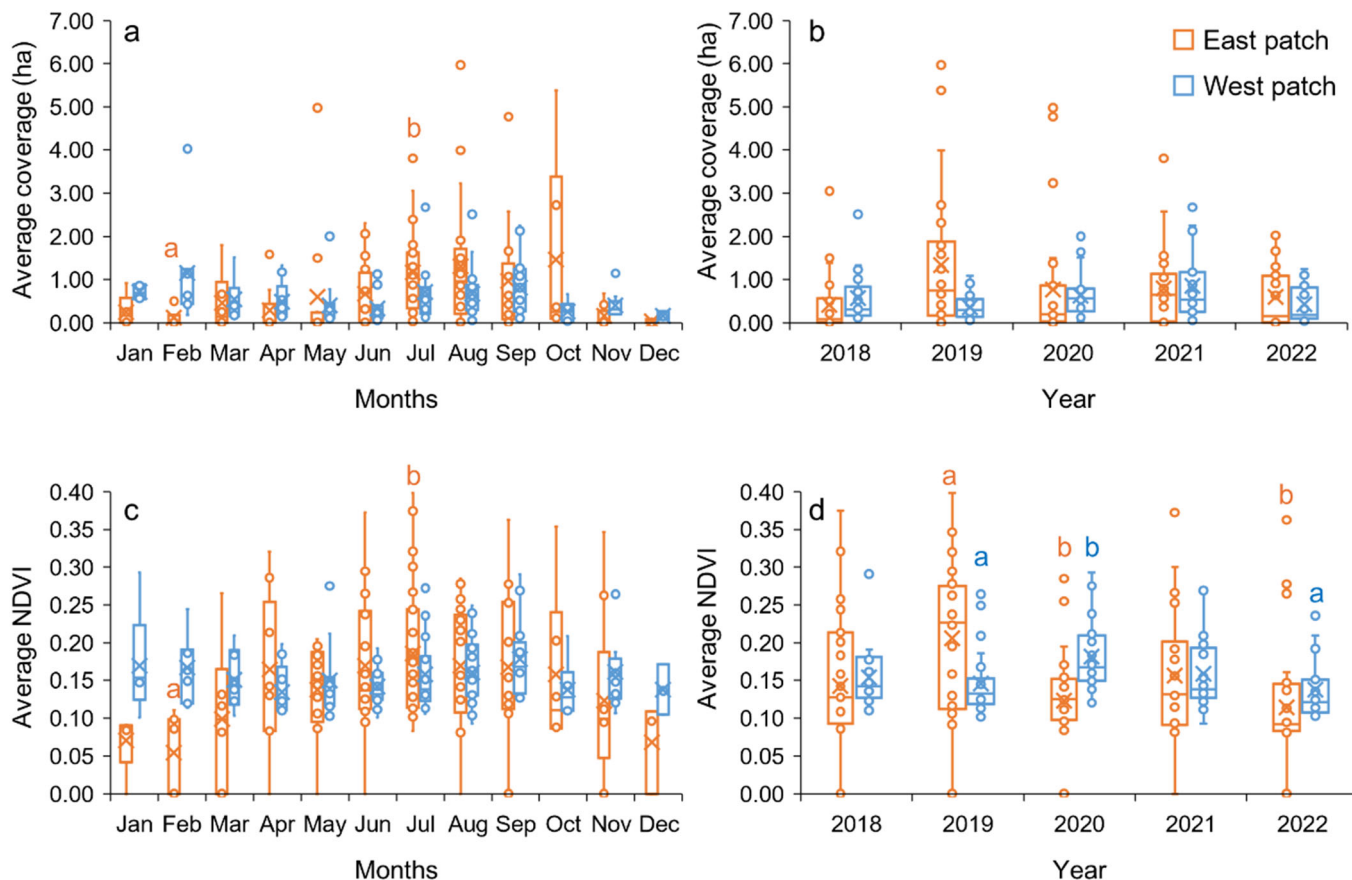


Figure 6. (a,b) Box plots showing monthly and annual averages of *R. okamurae* coverage for the eastern and western patches between 2018 and 2022. (c,d) Box plots showing monthly and annual averages of NDVI (used as a proxy of *R. okamurae* biomass washed ashore) for the eastern and western patches between 2018 and 2022. The east patch is plotted in orange, and the west patch in blue. The line within each box plot represents the median and the cross sign indicates the mean.

3.2. Spatiotemporal Distribution and Meteorological Variables

In Tarifa, the monthly average temperature for the period studied (2018–2022) ranged between 12 and 23 °C for January and August, respectively (Figure 7a). The months with the highest rainfall were March and April (80–100 mm of accumulated precipitation), while the lowest precipitation was recorded in July (0 mm) (Figure 7b). The prevailing wind directions were easterly and westerly, followed by south-westerly, with frequencies of 31%, 28%, and 11%, respectively, with minor variations between years (Table 1). Additionally, wind speeds reached up to 22 km h⁻¹ in May and September (REDIAM).

Table 1. Annual frequency (expressed as %) of the daily wind direction (north, N; northeast, NE; east, E; southeast, SE; south, S; southwest, SW; west, W; northwest, NW) at the meteorological station located in the municipality of Tarifa (Spain), from 2018 to 2022, as well as averaged across the period.

Wind Direction	2018	2019	2020	2021	2022	Average
N	0	1	1	1	20	5
NE	2	1	11	12	2	5
E	29	31	31	29	32	31
SE	4	5	7	6	7	6
S	6	7	8	8	6	7
SW	13	13	9	12	9	11
W	33	36	25	26	22	28
NW	4	3	3	5	2	4

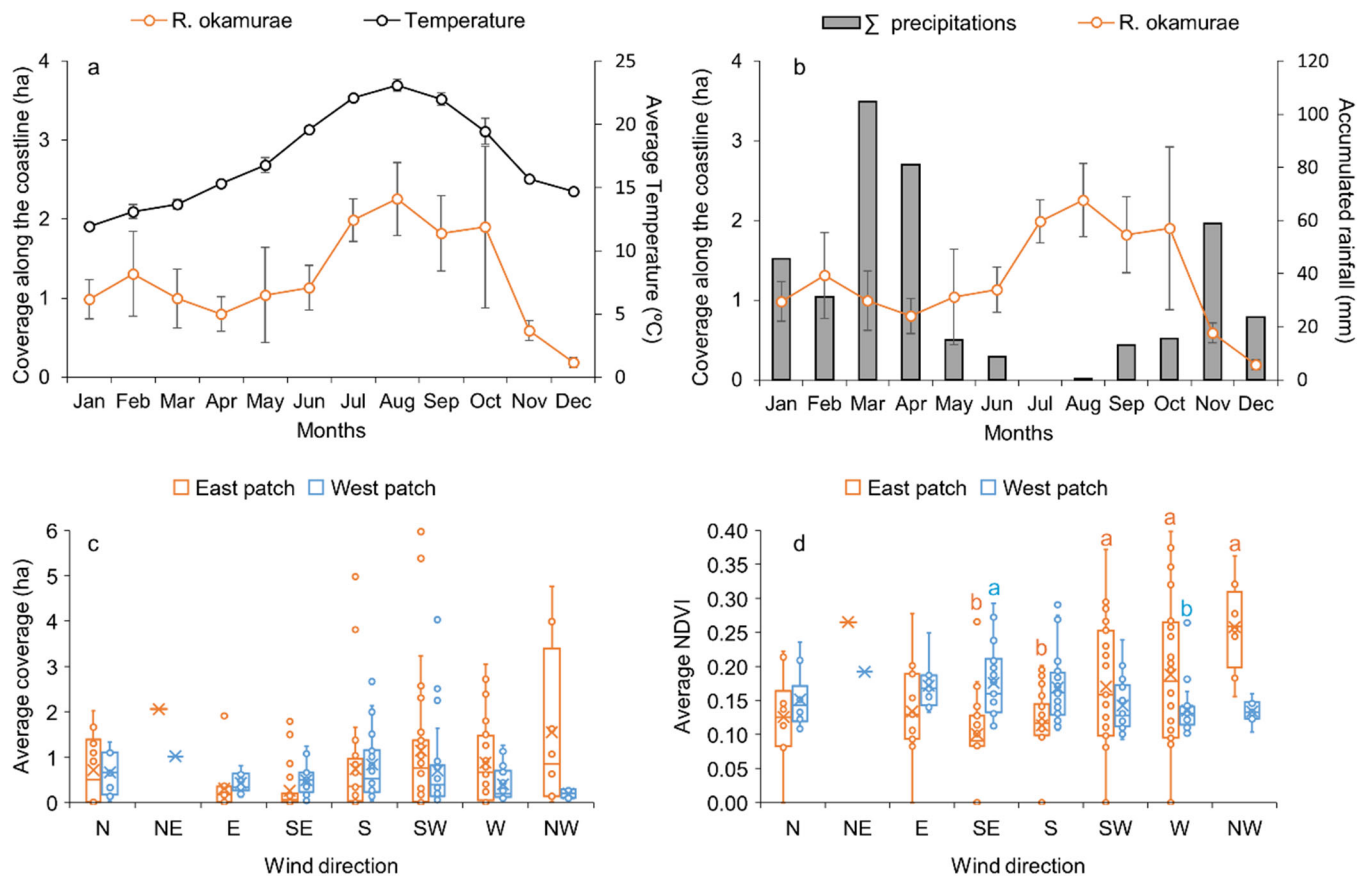


Figure 7. (a,b) Monthly average coverage of *R. okamurae* (ha) washed ashore for the entire coastline at Los Lances beach, compared with the monthly average air temperature (°C) and monthly accumulated precipitation (mm). Error bars indicate the standard error. (c,d) Box plots display the average coverage and NDVI of *R. okamurae* for both patches according to wind direction (north, N; northeast, NE; east, E; southeast, SE; south, S; southwest, SW; west, W; northwest, NW). The line within each box plot represents the median and the cross sign indicates the mean.

Significant Spearman correlations ($p < 0.05$; $n = 130$) between *R. okamurae* coverage and average NDVI across the entire coastline, as well as within the east and west patches, in relation to meteorological variables are presented in Table 2. A significant positive correlation was observed between the coverage and the average temperature for the 5 days prior to image acquisition (Spearman coefficient; rho = 0.301; $p < 0.001$, $n = 130$), and a significant negative correlation with accumulated precipitation (rho = -0.312; $p < 0.001$, $n = 130$) (Figure 7a,b). Additionally, accumulated rainfall and average temperature were significantly related to coverage and average NDVI in the eastern patch (Table 2). Significant correlations, inverse to each other, were found between coverage and average NDVI when analysed by patches. Specifically, the highest NDVI values in the west patch were associated with easterly and south-easterly winds (rho = -0.322; $p < 0.001$; $n = 130$). In contrast, in the east patch, higher average NDVI values were correlated with south-westerly and westerly winds (rho = +0.345; $p < 0.001$; $n = 130$) (Figure 7d). In addition, the average NDVI for both patches showed significant differences based on wind direction (p -value = 0.001; Kruskal-Wallis) (Figure 7d). Based on Figure 7d, significantly higher values were observed with south-westerly, westerly, and north-westerly winds for the eastern patch (p -adj. < 0.05 ; Dunn's post hoc test), while significant differences in the western patch were found between south-easterly and westerly winds (p -adj. < 0.05). However, no significant differences were observed in the coverage (Figure 7c). A significant positive correlation was found between the average NDVI for the west patch and wind speed (rho = 0.209; $p < 0.05$; $n = 130$).

Table 2. Significant Spearman coefficients (p -value < 0.05; $n = 130$) between *R. okamurae* coverage and average NDVI across the entire coastline, as well as for the east and west patches, in relation to accumulated rainfall, average temperature, wind direction, and wind speed for the 5 days prior to image acquisition.

Coverage for the Coastline	Average NDVI for the Coastline	East Patch Size	West Patch Size	Average NDVI for East Patch	Average NDVI for West Patch
Precipitation	−0.312	−0.214	−0.333	−0.241	
Temperature	0.301		0.332	0.184	0.223
Wind direction		0.238	0.216	−0.215	0.345
Wind speed					0.209

4. Discussion

4.1. Impact of Meteorological Conditions on *R. okamurae* Accumulation

Temperature seems to play a key role in the development and expansion of *R. okamurae* [6,27,60]. In Spain, the first strandings of *R. okamurae* were reported on the coast of Ceuta, in the summer of 2015. Actually, unusually high water surface temperatures in the summer of 2015, in July, were likely responsible for the proliferation of *R. okamurae* on the marine seabed of the Strait of Gibraltar [6,27]. Subsequently, golden tides of *R. okamurae* biomass were observed during the summer of 2017 at the beaches of Tarifa, Algeciras, and Ceuta [6], then quickly spreading along the coasts of Cadiz, Malaga, Granada and Almeria between 2016 and 2020 (*Catálogo Español de Especies Exóticas Invasoras—Algas*). In the current study, maximum levels of *R. okamurae* coverage along the entire coastline were recorded at Los Lances Beach in Tarifa during the summer months and early autumn (Figures 4a and 5), coinciding with the warm and dry periods (Figure 7a,b). Although significant seasonal variability in *R. okamurae* coverage was observed (Figure 4a), with the highest extent in August, unusual strandings were recorded on 28 August 2020, on the western patch of Los Lances beach (Figure 5b), and between 13 and 19 February 2023, at the beaches of the Algarve in southern Portugal [60]. Previously, strandings were reported in February 2018 on M'diq beach in the Alboran Sea, Morocco [27]. Despite these exceptions, the highest levels of *R. okamurae* beach-cast were related to elevated sea surface temperatures, which are very dependent on air temperature [60].

In the Pacific, *R. okamurae* is present all year round, although it becomes more abundant during the summer months as the thallus is reduced to a basal system of perennial rhizoids in the winter [17,61]. In winter, accumulated rainfall, lower temperatures, and reduced light penetration likely limit the growth of *R. okamurae*, a pattern typical of seaweed development in temperate coastal systems [62]. This could explain the significant negative correlation observed in our study between accumulated rainfall and the accumulation of *R. okamurae* biomass (with NDVI used as a proxy for biomass) along the entire coastline (Table 2). A hypothesis could be that *R. okamurae* reaches its maximum growth in early summer, and later drifts towards the coasts, as has been reported for other macrophytes in the Mediterranean [63]. The higher water temperatures reached during the summer months could favour the detachment of *R. okamurae* fragments (N. Korbee, oral communication, May 2024), increasing the *R. okamurae* golden tides in summer and early autumn. In fact, factors related to global warming (e.g., the rise in sea surface temperature) have likely exacerbated the proliferation of *R. okamurae* [6]. The rise in sea surface temperatures over the last two centuries could be favouring the expansion and impacts of marine non-native species [64,65], and algal species are shifting their distribution ranges in response to warming [66]. This process is being accelerated by human activities [67]. It was reported that tropical/subtropical macrophytes, including *R. okamurae*, could expand as they are not limited by the colder Mediterranean Sea surface temperature due to the plasticity of their lower thermal limit [68].

In addition to water temperature, which seems to be optimum for the growth of *R. okamurae* in the Strait of Gibraltar [27], wind speeds may influence biomass accumulation in the western patch (Table 2). Nevertheless, wind direction is the meteorological variable that seems to play a crucial role in biomass accumulation at both ends of the beach (Table 2), as indicated by Spearman coefficients showing inverse correlations between wind direction and average NDVI for each patch separately. This means that the westerly winds favour accumulation at the east patch, while easterly winds favour accumulation in the west patch (Figure 7d). In addition, the highest average NDVI values for the eastern patch were observed with southwesterly, westerly, and northwesterly winds, i.e., when the winds blew on-shore and northwesterly cross-shore (Figure S3). Conversely, the highest average NDVI values for the western patch were observed with southeasterly winds, i.e., when the winds blew in a southeasterly cross-shore direction (Figure S4). The role of wind direction in the accumulation of golden tides along the coastline was previously reported for *Ectocarpus* spp. in Dublin Bay (Ireland) and *Sargassum* spp. in the Caribbean [4,44]. For this reason, forecasting wind direction could be useful for planning of intensive removal of algal biomass from the coast in summer and early autumn.

Significant annual differences observed in average NDVI for both patches could be due to variations in the annual frequency of wind directions (Figure 6d). Concretely in Tarifa, during the studied period (2018–2022), the prevailing wind directions were easterly and westerly, followed by south-westerly, with frequencies of 31%, 28%, and 11%, respectively (Table 1; Figure S5). In this sense, the significant decrease in NDVI in the patch located at the eastern end during 2020 and 2022 could be due to the higher frequency of south-westerly winds during 2019 compared to 2020 and 2022 (13% versus 9%). Conversely, in 2020, south-easterly winds were slightly more frequent, favouring the accumulation of strandings in the west patch. However, these annual differences, particularly the decrease in the eastern patch in 2022, could also be due to the mechanical removal of biomass strandings by the local administration, which has increased in recent years. Thus, the coverage and biomass of *R. okamurae* invasive seaweed strandings could be underestimated during the summer months when the algal biomass strandings are mechanically removed early in the morning before the Sentinel-2 overflight of the study area. It is important to highlight that, according to the summer timetable, Sentinel-2 overflies the study area at approximately 1 p.m.

4.2. Strategies for Enhanced Management and Removal of *R. okamurae* Strandings

The *R. okamurae* biomass collection should ideally be executed at sea prior to washing ashore. This approach would not only improve the quality of the biomass for potential use (e.g., composting, bioplastics, and cosmetic applications) but also reduce the loss of beach sand associated with cleaning operations [33,46]. It has been estimated that approximately 10% of the volume removed during *Posidonia oceanica* strandings on a Sardinian beach (Italy) consisted of sand [42]. Given the physical characteristics of *R. okamurae* in comparison with the simpler morphology of *P. oceanica*, it is reasonable to expect that this percentage could be even higher when mechanically removing this seaweed.

The mechanical removal operations conducted by the Tarifa City Council have increased in recent years, which might explain the lower *R. okamurae* biomass washed ashore that was observed in 2022 (Figure 4d). Unfortunately, the algal biomass removed mechanically is not systematically quantified, and only occasional measurements have been conducted. Furthermore, mechanical removal operations are more frequent during the summer months (i.e., July–September, [34]), which can also contribute to the lack of a clear seasonal pattern in the *R. okamurae* algal biomass along the coastline (i.e., average NDVI; Figure 4c). Therefore, documenting the quantity of algal biomass removed could enhance our knowledge and understanding of this challenge and support the development of improved management strategies.

Removing floating *R. okamurae* before it reaches the shore is crucial as it prevents the spread of highly invasive, photosynthetically active fragments. Unfortunately, it is likely that *R. okamurae* cannot be eradicated [12]; however, measures such as the removal

of floating algal biomass could help limit the expansion of this invasive species. This species lacks natural predators, a key factor that facilitates its rapid growth and spread [40]. The invasive potential of *R. okamurae* is significantly enhanced by its ability to reattach its floating fragments to substrates, enabling rapid expansion across new areas [69]. This characteristic emphasizes the need for thorough monitoring and management strategies across all coastal zones—both intertidal and subtidal. Furthermore, external factors such as nutrient inputs enhance the growth of *R. okamurae*, leading to more frequent strandings along coastlines [6,28]. Secondary water flows have also been identified as crucial in understanding the initial spread of this invasive seaweed through the coastal systems of the Alboran Sea and the Strait of Gibraltar [70]. Future studies should consider in greater depth the role of marine currents as potential environmental drivers of *R. okamurae* golden tides, which could be important for establishing strategies for the enhanced management of *R. okamurae* stranding. However, at present, no coastal data of sufficient quality are available for incorporation into the analysis in this region. The radar altimeter data from Copernicus or other programmes do not have sufficient resolution to accurately monitor coastal currents in this location, particularly at Los Lances beach, due to the complexity of tidal currents and the proximity to the coast [71,72]. During the initial phase of this study, tidal coefficients [i.e., fortnightly tidal cycles (spring and neap tides)] were considered as a proxy of tidal current intensity. Spearman coefficients between tidal coefficients and coverage, as well as average NDVI for the entire coastline and both patches, were not significant, except for coverage in the western patch ($\rho = 0.208$; p -value = 0.018; $n = 130$). Nevertheless, significant differences between daily tidal coefficients (very high, high, medium, and low) were not found ($X^2 = 6.94$, $df = 3$, p -value = 0.07; Kruskal-Wallis).

The invasive seaweed *R. okamurae* is one of the main challenges facing southern European coastal ecosystems of the Mediterranean Sea, and potentially the Atlantic Ocean [22]. To manage its spread effectively, a multidisciplinary approach is necessary, integrating ecological insights with practical management strategies. This study presents an approach focused on monitoring the strandings of *R. okamurae* accumulated on the beach from 2015 onwards using Sentinel-2 imagery. This method, which may be applicable in other coastal regions globally, has the potential to provide valuable information for designing management plans aimed at reducing the costs of maintaining clean coasts. It is important to highlight that the BioIntertidal Mapper software (v1; developed for mapping golden tides among other photosynthetic organisms) can be employed to monitor *R. okamurae* golden tides along the shoreline in the absence of other macrophytes [73]. This user-friendly tool might facilitate the work of governmental regulatory agencies, allowing for extensive monitoring and the adoption of standardized protocols across geographic areas with minimal costs. Furthermore, future efforts must focus on both monitoring and managing this invasive species to mitigate its impact, protect marine biodiversity, and support local economies dependent on these coastal environments. Finally, to fully address this environmental and socio-economic challenge, it is essential to develop more effective management strategies. This includes methodologies of analysis such as machine learning, deep learning, and artificial intelligence, along with EO data processing that will allow for the monitoring of the invasive *R. okamurae* seaweed as it attaches to substrates in supratidal zones, floats in intertidal zones, and washes ashore. Meanwhile, this study presents an approach that simplifies and facilitates the long-term identification of brown seaweeds washed ashore. It would be interesting to explore whether the outputs from this approach, combined with smart monitoring techniques [74,75], could enhance the training of artificial intelligence algorithms, or even digital twins. This could specifically aid in identifying the different stages of this brown seaweed invasion (attachment to substrates, floating, and washed ashore) and analysing potential environmental drivers that predict golden tides in the distant future.

5. Conclusions

In this study, a validated method was applied for mapping golden tides (specifically the invasive brown algae *R. okamurae*) along the shoreline using freely accessible satellite images with a spatial resolution of 10 m. The spatial and temporal variability of *R. okamurae* strandings (coverage and average NDVI) along the coast were assessed over a five-year period (2018–2022), revealing significant massive accumulations during summer and early autumn, along with spatial differences. The most favourable meteorological conditions for the arrival of strandings on the coast (in this case, average temperature, accumulated rainfall, and wind direction) were also identified. These findings have provided crucial insights for the development of strategies to manage and mitigate the impact of invasive seaweed strandings on coastal ecosystems worldwide.

Supplementary Materials: The following supporting information can be downloaded at <https://www.mdpi.com/article/10.3390/rs16152689/s1>: Figure S1: photos of *R. okamurae* golden tides on Los Lances beach; Figure S2: coverage and NDVI (values above 0.08) associated with golden tides (i.e., brown seaweed strandings) of *Rugulopteryx okamurae* along the coastline on Bolonia Beach (Tarifa, Cadiz, Spain) on 30 June 2021; Figure S3: box plots displaying the average NDVI of *R. okamurae* for eastern patch of the Los Lances Beach (Tarifa, Cadiz, Spain) according to wind direction; Figure S4: box plots displaying the average NDVI of *R. okamurae* for western patch of the Los Lances Beach (Tarifa, Cadiz, Spain) according to wind direction; Figure S5: frequency (expressed as %) of the daily wind direction at the meteorological station located in the municipality of Tarifa (Spain), from 2018 to 2022, as well as averaged across the period.

Author Contributions: S.H.: conceptualization, data curation, formal analysis, funding acquisition, investigation, methodology, software, validation, visualization, writing—original draft; L.M.: funding acquisition, supervision, writing—review and editing; I.C.: conceptualization, funding acquisition, supervision, visualization, writing—review and editing; F.L.F.: funding acquisition, writing—review and editing; N.K.: funding acquisition, writing—review and editing; G.N.: conceptualization, visualization, writing—review and editing; R.B.: conceptualization, funding acquisition, investigation, supervision, writing—review and editing. All authors have read and agreed to the published version of the manuscript.

Funding: This project was funded by a postdoctoral fellowship from the Fundación Ramón Areces “XXXIII Call for Further Studies Abroad in Life and Material Sciences”. Additionally, the research activities received funding from the H2020 European project CLIMAREST (Grant Agreement ID: 101093865), the BLUEMARO project (PID2020-116136RB-I00), supported by the Ministry of Science and Innovation of Spain, and the grant CNS2023-143630, funded by MICIU/AEI/10.13039/501100011033 and the European Union’s Next Generation EU/PRTR.

Data Availability Statement: Data generated and used during the study have been uploaded on the figshare repository and are available at <https://figshare.com/s/d784f7cac8ad6f14af2e> (accessed on 22 July 2024). Sample codes used for the processing and analysis are available at <https://github.com/sharpe/Assessing-Golden-Tides-from-Space> (accessed on 17 July 2024).

Acknowledgments: We thank the European Commission’s Copernicus program for distributing Sentinel-2 imagery.

Conflicts of Interest: The authors declare that they have no known competing financial interests or personal relationships that could have appeared to influence the work reported in this paper.

References

1. Smetacek, V.; Zingone, A. Green and Golden Seaweed Tides on the Rise. *Nature* **2013**, *504*, 84–88. [[CrossRef](#)] [[PubMed](#)]
2. Wang, M.; Hu, C. Mapping and Quantifying Sargassum Distribution and Coverage in the Central West Atlantic Using MODIS Observations. *Remote Sens. Environ.* **2016**, *183*, 350–367. [[CrossRef](#)]
3. Jeffrey, D.W.; Madden, B.; Rafferty, B. Beach Fouling by Ectocarpus Siliculosus in Dublin Bay. *Mar. Pollut. Bull.* **1993**, *26*, 51–53. [[CrossRef](#)]
4. Haro, S.; Bermejo, R.; Wilkes, R.; Bull, L.; Morrison, L. Monitoring Intertidal Golden Tides Dominated by Ectocarpus Siliculosus Using Sentinel-2 Imagery. *Int. J. Appl. Earth Obs. Geoinf.* **2023**, *122*, 103451. [[CrossRef](#)]

5. Zárate, R.; Portillo, E.; Teixidó, S.; de Carvalho, M.A.A.P.; Nunes, N.; Ferraz, S.; Seca, A.M.L.; Rosa, G.P.; Barreto, M.C. Pharmacological and Cosmeceutical Potential of Seaweed Beach-Casts of Macaronesia. *Appl. Sci.* **2020**, *10*, 5831. [[CrossRef](#)]
6. García-Gómez, J.C.; Sempere-Valverde, J.; González, A.R.; Martínez-Chacón, M.; Olaya-Ponzone, L.; Sánchez-Moyano, E.; Ostalé-Valriberas, E.; Megina, C. From Exotic to Invasive in Record Time: The Extreme Impact of *Rugulopteryx okamurae* (Dictyotales, Ochrophyta) in the Strait of Gibraltar. *Sci. Total Environ.* **2020**, *704*, 135408. [[CrossRef](#)] [[PubMed](#)]
7. Schaffelke, B.; Hewitt, C.L. Impacts of Introduced Seaweeds. *Bot. Mar.* **2007**, *50*, 397–417. [[CrossRef](#)]
8. Bermejo, R.; Green-Gavrielidis, L.; Gao, G. Editorial: Macroalgal Blooms in a Global Change Context. *Front. Mar. Sci.* **2023**, *10*, 1204117. [[CrossRef](#)]
9. Valiela, I.; McClelland, J.; Hauxwell, J.; Behr, P.J.; Hersh, D.; Foreman, K. Macroalgal Blooms in Shallow Estuaries: Controls and Ecophysiological and Ecosystem Consequences. *Limnol. Oceanogr.* **1997**, *42*, 1105–1118. [[CrossRef](#)]
10. Bermejo, R.; MacMonagail, M.; Heesch, S.; Mendes, A.; Edwards, M.; Fenton, O.; Knöller, K.; Daly, E.; Morrison, L. The Arrival of a Red Invasive Seaweed to a Nutrient Over-Enriched Estuary Increases the Spatial Extent of Macroalgal Blooms. *Mar. Environ. Res.* **2020**, *158*, 104944. [[CrossRef](#)] [[PubMed](#)]
11. Yoshida, G.; Uchimura, M.; Hiraoka, M. Persistent Occurrence of Floating *Ulva* Green Tide in Hiroshima Bay, Japan: Seasonal Succession and Growth Patterns of *Ulva* Pertusa and *Ulva* spp. (Chlorophyta, Ulvales). *Hydrobiologia* **2015**, *758*, 223–233. [[CrossRef](#)]
12. Anderson, L.W.J. Control of Invasive Seaweeds. *Bot. Mar.* **2007**, *50*, 418–437. [[CrossRef](#)]
13. Thomsen, M.S.; Ramus, A.P.; Long, Z.T.; Silliman, B.R. A Seaweed Increases Ecosystem Multifunctionality When Invading Bare Mudflats. *Biol. Invasions* **2019**, *21*, 27–36. [[CrossRef](#)]
14. Critchley, A.T.; Farnham, W.F.; Morrell, S.L. An Account of the Attempted Control of an Introduced Marine Alga, *Sargassum Muticum*, in Southern England. *Biol. Conserv.* **1986**, *35*, 313–332. [[CrossRef](#)]
15. South, P.M.; Floerl, O.; Forrest, B.M.; Thomsen, M.S. A Review of Three Decades of Research on the Invasive Kelp *Undaria Pinnatifida* in Australasia: An Assessment of Its Success, Impacts and Status as One of the World's Worst Invaders. *Mar. Environ. Res.* **2017**, *131*, 243–257. [[CrossRef](#)] [[PubMed](#)]
16. Anderson, L.W.J. California's Reaction to *Caulerpa Taxifolia*: A Model for Invasive Species Rapid Response. *Biol. Invasions* **2005**, *7*, 1003–1016. [[CrossRef](#)]
17. Hwang, I.-K.; Lee, W.J.; Kim, H.-S.; De Clerck, O. Taxonomic Reappraisal of *Dilophus okamurae* (Dictyotales, Phaeophyta) from the Western Pacific Ocean. *Phycologia* **2009**, *48*, 1–12. [[CrossRef](#)]
18. Verlaque, M.; Steen, F.; De Clerck, O. *Rugulopteryx* (Dictyotales, Phaeophyceae), a Genus Recently Introduced to the Mediterranean. *Phycologia* **2009**, *48*, 536–542. [[CrossRef](#)]
19. Ruitton, S.; Blanfuné, A.; Boudouresque, C.-F.; Guillemain, D.; Michotey, V.; Roblet, S.; Thibault, D.; Thibaut, T.; Verlaque, M.; Rodríguez, C. Rapid Spread of the Invasive Brown Alga *Rugulopteryx okamurae* in a National Park in Provence (France, Mediterranean Sea). *Water* **2021**, *13*, 2306. [[CrossRef](#)]
20. Altamirano, M.; De la Rosa Álamos, J.; Martínez Medina, F.J. Arribazones de La Especie Exótica *Rugulopteryx okamurae* (E.Y. Dawson) I.K. Hwang, W.J. Lee & H.S. Kim (Dictyotales, Ochrophyta) En El Estrecho de Gibraltar: Primera Cita Para El Atlántico y España. *Algas* **2016**, *52*, 20.
21. Ocaña, Ó.; Afonso Carrillo, J.; Ballesteros, E. Massive Proliferation of a Dictyotalean Species (Phaeophyceae, Ochrophyta) through the Strait of Gibraltar (Research Note). *Rev. la Acad. Canar. Ciencias* **2016**, *28*, 165–170.
22. Mateo-Ramírez, Á.; Iñiguez, C.; Fernández-Salas, L.M.; Sánchez-Leal, R.F.; Farias, C.; Bellanco, M.J.; Gil, J.; Rueda, J.L. Healthy Thalli of the Invasive Seaweed *Rugulopteryx okamurae* (Phaeophyceae) Being Massively Dragged into Deep-Sea Bottoms by the Mediterranean Outflow Water. *Phycologia* **2023**, *62*, 99–108. [[CrossRef](#)]
23. Faria, J.; Prestes, A.C.L.; Moreu, I.; Martins, G.M.; Neto, A.I.; Cacabelos, E. Arrival and Proliferation of the Invasive Seaweed *Rugulopteryx okamurae* in NE Atlantic Islands. *Bot. Mar.* **2022**, *65*, 45–50. [[CrossRef](#)]
24. Terradas-Fernández, M.; Pena-Martín, C.; Valverde-Urrea, M.; Gran, A.; Blanco-Murillo, F.; Leyva, L.; Abellán-Gallardo, E.; Beresaluz, E.; Izquierdo, A.; del Pilar-Ruso, Y.; et al. An Outbreak of the Invasive Macroalgae *Rugulopteryx okamurae* in Alicante Bay and Its Colonization on Dead *Posidonia Oceanica* Matte. *Aquat. Bot.* **2023**, *189*, 103706. [[CrossRef](#)]
25. El Madany, M.; Hassoun, M.; El Aamri, F.; El Mtili, N. Recent Occurrence and Expansion of the Non-Indigenous Alga *Rugulopteryx okamurae* in Morocco (Mediterranean and Atlantic Shores). *Aquat. Bot.* **2024**, *190*, 103722. [[CrossRef](#)]
26. Bellissimo, G.; Altamirano, M.; Muñoz, A.; De la Rosa, J.; Hung, T.H.; Rizzuto, G.; Vizzini, S.; Tomasello, A. The Invasive Brown Seaweed *Rugulopteryx okamurae* (Dictyotales, Ochrophyta) Continues to Expand: First Record in Italy. *BioInvasions Rec.* **2024**, *13*, 385–401. [[CrossRef](#)]
27. El Aamri, F.; Idhalla, M.; Tamsouri, M.N. Occurrence of the Invasive Brown Seaweed *Rugulopteryx okamurae* (E.Y. Dawson) I.K. Hwang, W.J. Lee & H.S. Kim (Dictyotales, Phaeophyta) in Morocco (Mediterranean Sea). *Mediterr. Fish. Aquac. Res.* **2018**, *1*, 92–96.
28. Mercado, J.M.; Gómez-Jakobsen, F.; Korbee, N.; Aviles, A.; Bonomi-Barufi, J.; Muñoz, M.; Reul, A.; Figueroa, F.L. Analyzing Environmental Factors That Favor the Growth of the Invasive Brown Macroalga *Rugulopteryx okamurae* (Ochrophyta): The Probable Role of the Nutrient Excess. *Mar. Pollut. Bull.* **2022**, *174*, 113315. [[CrossRef](#)] [[PubMed](#)]
29. Faria, J.; Prestes, A.C.L.; Moreu, I.; Cacabelos, E.; Martins, G.M. Dramatic Changes in the Structure of Shallow-Water Marine Benthic Communities Following the Invasion by *Rugulopteryx okamurae* (Dictyotales, Ochrophyta) in Azores (NE Atlantic). *Mar. Pollut. Bull.* **2022**, *175*, 113358. [[CrossRef](#)] [[PubMed](#)]

30. Azcárate-García, T.; Beca-Carretero, P.; Brun, F.G. Plant and Meadow Structure Characterisation of *Posidonia Oceanica* in Its Westernmost Distribution Range. *Diversity* **2023**, *15*, 101. [[CrossRef](#)]
31. Figueroa, F.L.; Sesmero, R.; Arijo, S. Interdisciplinar Research (Oceanography, Botany, Ecophysiology and Biotechnology) about the Invasive Exotic Species *Rugulopteryx okamurae* (Ochrophyta), in the Frame of the Project “BLUEMARO”. *Memorias la Real Soc. Española Hist. Nat.* **2023**, *16*, 9–29.
32. Sempere-Valverde, J.; Ostalé-Valriberas, E.; Maestre, M.; González Aranda, R.; Bazairi, H.; Espinosa, F. Impacts of the Non-Indigenous Seaweed *Rugulopteryx okamurae* on a Mediterranean Coralligenous Community (Strait of Gibraltar): The Role of Long-Term Monitoring. *Ecol. Indic.* **2021**, *121*, 107135. [[CrossRef](#)]
33. Mogollón, S.L.; Zilio, M.I.; Buitrago, E.M.; Caraballo, M.Á.; Yñiguez, R. Economic Impact of *Rugulopteryx okamurae* (Dictyotales, Ochrophyta) along the Andalusian Coastline: The Case of Tarifa, Spain. *Wetl. Ecol. Manag.* **2024**, *32*, 19–32. [[CrossRef](#)]
34. Ayuntamiento de Tarifa. *Informe Sobre Las Actuaciones Realizadas En La Playa de Los Lances Sur y Playa de Atlanterra Ante La Acumulación Masiva de Algas En El Litoral Tarifeño. Verano 2021*; Ayuntamiento de Tarifa: Tarifa, Spain, 2021; pp. 1–4.
35. Wan, A.H.L.; Wilkes, R.J.; Heesch, S.; Bermejo, R.; Johnson, M.P.; Morrison, L. Assessment and Characterisation of Ireland’s Green Tides (Ulva Species). *PLoS ONE* **2017**, *12*, e0169049. [[CrossRef](#)] [[PubMed](#)]
36. Joniver, C.F.H.; Photiades, A.; Moore, P.J.; Winters, A.L.; Woolmer, A.; Adams, J.M.M. The Global Problem of Nuisance Macroalgal Blooms and Pathways to Its Use in the Circular Economy. *Algal Res.* **2021**, *58*, 102407. [[CrossRef](#)]
37. Harb, T.B.; Vega, J.; Bonomi-Barufi, J.; Casas, V.; Abdala-Díaz, R.; Figueroa, F.L.; Chow, F. Brazilian Beach-Cast Seaweeds: Antioxidant, Photoprotection and Cytotoxicity Properties. *Waste Biomass Valorization* **2023**, *14*, 2249–2265. [[CrossRef](#)]
38. Pereira, A.G.; Fraga-Corral, M.; Garcia-Oliveira, P.; Lourenço-Lopes, C.; Carpêna, M.; Prieto, M.A.; Simal-Gandara, J. The Use of Invasive Algae Species as a Source of Secondary Metabolites and Biological Activities: Spain as Case-Study. *Mar. Drugs* **2021**, *19*, 178. [[CrossRef](#)] [[PubMed](#)]
39. Pereira, L. Non-Indigenous Seaweeds in the Iberian Peninsula, Macaronesia Islands (Madeira, Azores, Canary Islands) and Balearic Islands: Biodiversity, Ecological Impact, Invasion Dynamics, and Potential Industrial Applications. *Algal Res.* **2024**, *78*, 103407. [[CrossRef](#)]
40. Casal-Porras, I.; Zubía, E.; Brun, F.G. Dilkamural: A Novel Chemical Weapon Involved in the Invasive Capacity of the Alga *Rugulopteryx okamurae* in the Strait of Gibraltar. *Estuar. Coast. Shelf Sci.* **2021**, *257*, 107398. [[CrossRef](#)]
41. Patón, D.; García-Gómez, J.C.; Loring, J.; Torres, A. Composting the Invasive Toxic Seaweed *Rugulopteryx okamurae* Using Five Invertebrate Species, and a Mini-Review on Composting Macroalgae. *Waste Biomass Valorization* **2023**, *14*, 167–184. [[CrossRef](#)]
42. Manca, E.; Pascucci, V.; Deluca, M.; Cossu, A.; Andreucci, S. Shoreline Evolution Related to Coastal Development of a Managed Beach in Alghero, Sardinia, Italy. *Ocean Coast. Manag.* **2013**, *85*, 65–76. [[CrossRef](#)]
43. Kiirikki, M.; Blomster, J. Wind Induced Upwelling as a Possible Explanation for Mass Occurrences of Epiphytic Ectocarpus Siliculosus (Phaeophyta) in the Northern Baltic Proper. *Mar. Biol.* **1996**, *127*, 353–358. [[CrossRef](#)]
44. Robledo, D.; Vázquez-Delfín, E.; Freile-Pelegrín, Y.; Vásquez-Elizondo, R.M.; Qui-Minet, Z.N.; Salazar-Garibay, A. Challenges and Opportunities in Relation to Sargassum Events Along the Caribbean Sea. *Front. Mar. Sci.* **2021**, *8*, 699664. [[CrossRef](#)]
45. Finch, D.M.; Butler, J.L.; Runyon, J.B.; Fettig, C.J.; Kilkenny, F.F.; Jose, S.; Frankel, S.J.; Cushman, S.A.; Cobb, R.C.; Dukes, J.S.; et al. Effects of Climate Change on Invasive Species. In *Invasive Species in Forests and Rangelands of the United States*; Springer International Publishing: Cham, Switzerland, 2021; pp. 57–83; ISBN 978-3-030-45366-4.
46. Barcellos, L.; Pham, C.K.; Menezes, G.; Bettencourt, R.; Rocha, N.; Carvalho, M.; Felgueiras, H.P. A Concise Review on the Potential Applications of *Rugulopteryx okamurae* Macroalgae. *Mar. Drugs* **2023**, *21*, 40. [[CrossRef](#)] [[PubMed](#)]
47. Vega, J.; Catalá, T.S.; García-Márquez, J.; Speidel, L.G.; Arijo, S.; Cornelius Kunz, N.; Geisler, C.; Figueroa, F.L. Molecular Diversity and Biochemical Content in Two Invasive Alien Species: Looking for Chemical Similarities and Bioactivities. *Mar. Drugs* **2022**, *21*, 5. [[CrossRef](#)] [[PubMed](#)]
48. Xiao, J.; Wang, Z.; Liu, D.; Fu, M.; Yuan, C.; Yan, T. Harmful Macroalgal Blooms (HMBs) in China’s Coastal Water: Green and Golden Tides. *Harmful Algae* **2021**, *107*, 102061. [[CrossRef](#)] [[PubMed](#)]
49. Qi, L.; Hu, C. To What Extent Can Ulva and Sargassum Be Detected and Separated in Satellite Imagery? *Harmful Algae* **2021**, *103*, 102001. [[CrossRef](#)] [[PubMed](#)]
50. Xiao, Y.; Liu, R.; Kim, K.; Zhang, J.; Cui, T. A Random Forest-Based Algorithm to Distinguish *Ulva prolifera* and *Sargassum* From Multispectral Satellite Images. *IEEE Trans. Geosci. Remote Sens.* **2022**, *60*, 4201515. [[CrossRef](#)]
51. Wang, M.; Hu, C. Satellite Remote Sensing of Pelagic Sargassum Macroalgae: The Power of High Resolution and Deep Learning. *Remote Sens. Environ.* **2021**, *264*, 112631. [[CrossRef](#)]
52. Laval, M.; Belmouhcine, A.; Courtrai, L.; Descloires, J.; Salazar-Garibay, A.; Schamberger, L.; Minghelli, A.; Thibaut, T.; Dorville, R.; Mazoyer, C.; et al. Detection of Sargassum from Sentinel Satellite Sensors Using Deep Learning Approach. *Remote Sens.* **2023**, *15*, 1104. [[CrossRef](#)]
53. Lazcano-Hernandez, H.E.; Arellano-Verdejo, J.; Rodríguez-Martínez, R.E. Algorithms Applied for Monitoring Pelagic Sargassum. *Front. Mar. Sci.* **2023**, *10*, 1216426. [[CrossRef](#)]
54. Roca, M.; Dunbar, M.B.; Román, A.; Caballero, I.; Zoffoli, L.M.; Gernez, P.; Navarro, G. Monitoring the Marine Invasive Alien Species *Rugulopteryx okamurae* Using Unmanned Aerial Vehicles and Satellites. *Front. Mar. Sci.* **2022**, *9*, 1004012. [[CrossRef](#)]
55. Rudin, C. Stop Explaining Black Box Machine Learning Models for High Stakes Decisions and Use Interpretable Models Instead. *Nat. Mach. Intell.* **2019**, *1*, 206–215. [[CrossRef](#)] [[PubMed](#)]

56. Rueda, J.L.; Mena-Torres, A.; Gallardo-Núñez, M.; González-García, E.; Martín-Arjona, A.; Valenzuela, J.; García-Ruiz, C.; González-Aguilar, M.; Mateo-Ramírez, Á.; García, M.; et al. Spatial Distribution and Potential Impact of Drifted Thalli of the Invasive Alga *Rugulopteryx okamurae* in Circalittoral and Bathyal Habitats of the Northern Strait of Gibraltar and the Alboran Sea. *Diversity* **2023**, *15*, 1206. [[CrossRef](#)]
57. Zoffoli, L.M.; Gernez, P.; Rosa, P.; Le, A.; Brando, V.E.; Barillé, A.; Harin, N.; Peters, S.; Poser, K.; Spaias, L.; et al. Remote Sensing of Environment Sentinel-2 Remote Sensing of Zostera Noltii-Dominated Intertidal Seagrass Meadows. *Remote Sens. Environ.* **2020**, *251*, 112020. [[CrossRef](#)]
58. Haro, S.; Jesus, B.; Oiry, S.; Papaspyrou, S.; Lara, M.; González, C.J.; Corzo, A. Microphytobenthos Spatio-Temporal Dynamics across an Intertidal Gradient Using Random Forest Classification and Sentinel-2 Imagery. *Sci. Total Environ.* **2022**, *804*, 149983. [[CrossRef](#)] [[PubMed](#)]
59. Karki, S.; Bermejo, R.; Wilkes, R.; Monagail, M.M.; Daly, E.; Healy, M.; Hanafin, J.; McKinstry, A.; Mellander, P.-E.; Fenton, O.; et al. Mapping Spatial Distribution and Biomass of Intertidal Ulva Blooms Using Machine Learning and Earth Observation. *Front. Mar. Sci.* **2021**, *8*, 633128. [[CrossRef](#)]
60. Herrero, J.J.; Simes, D.C.; Abecasis, R.; Relvas, P.; Garel, E.; Ventura Martins, P.; Santos, R. Monitoring Invasive Macroalgae in Southern Portugal: Drivers and Citizen Science Contribution. *Front. Environ. Sci.* **2023**, *11*, 1324600. [[CrossRef](#)]
61. García-Gómez, J.C.; Florido, M.; Olaya-Ponzone, L.; Rey Díaz de Rada, J.; Donázar-Aramendía, I.; Chacón, M.; Quintero, J.J.; Magariño, S.; Megina, C. Monitoring Extreme Impacts of *Rugulopteryx okamurae* (Dictyotales, Ochrophyta) in El Estrecho Natural Park (Biosphere Reserve). Showing Radical Changes in the Underwater Seascape. *Front. Ecol. Evol.* **2021**, *9*, 639161. [[CrossRef](#)]
62. Bermejo, R.; Golden, N.; Schrofner, E.; Knöller, K.; Fenton, O.; Serrão, E.; Morrison, L. Biomass and Nutrient Dynamics of Major Green Tides in Ireland: Implications for Biomonitoring. *Mar. Pollut. Bull.* **2022**, *175*, 113318. [[CrossRef](#)]
63. Bermejo, R.; de la Fuente, G.; Vergara, J.J.; Hernández, I. Application of the CARLIT Index along a Biogeographical Gradient in the Alboran Sea (European Coast). *Mar. Pollut. Bull.* **2013**, *72*, 107–118. [[CrossRef](#)] [[PubMed](#)]
64. Hellmann, J.J.; Byers, J.E.; Bierwagen, B.G.; Dukes, J.S. Five Potential Consequences of Climate Change for Invasive Species. *Conserv. Biol.* **2008**, *22*, 534–543. [[CrossRef](#)] [[PubMed](#)]
65. Walther, G.-R.; Roques, A.; Hulme, P.E.; Sykes, M.T.; Pyšek, P.; Kühn, I.; Zobel, M.; Bacher, S.; Botta-Dukát, Z.; Bugmann, H. Alien Species in a Warmer World: Risks and Opportunities. *Trends Ecol. Evol.* **2009**, *24*, 686–693. [[CrossRef](#)] [[PubMed](#)]
66. Pecl, G.T.; Araújo, M.B.; Bell, J.D.; Blanchard, J.; Bonebrake, T.C.; Chen, I.-C.; Clark, T.D.; Colwell, R.K.; Danielsen, F.; Evengård, B.; et al. Biodiversity Redistribution under Climate Change: Impacts on Ecosystems and Human Well-Being. *Science* **2017**, *355*, eaai9214. [[CrossRef](#)] [[PubMed](#)]
67. Blackburn, T.M.; Pyšek, P.; Bacher, S.; Carlton, J.T.; Duncan, R.P.; Jarošík, V.; Wilson, J.R.U.; Richardson, D.M. A Proposed Unified Framework for Biological Invasions. *Trends Ecol. Evol.* **2011**, *26*, 333–339. [[CrossRef](#)] [[PubMed](#)]
68. Wesselmann, M.; Hendriks, I.E.; Johnson, M.; Jordà, G.; Mineur, F.; Marbà, N. Increasing Spread Rates of Tropical Non-native Macrophytes in the Mediterranean Sea. *Glob. Chang. Biol.* **2024**, *30*, e17249. [[CrossRef](#)] [[PubMed](#)]
69. Figueroa, F.L.; Vega, J.V.; Valderrama, M.G.; Flores-Moya, A. Invasión de La Especie Exótica *Rugulopteryx okamurae* En Andalucía I: Estudios Preliminares de La Actividad Fotosintética. *Algas* **56**. Boletín la Soc. Española Ficología **2020**, *56*, 35–46.
70. García-Lafuente, J.; Nadal, I.; Sammartino, S.; Korbee, N.; Figueroa, F.L. Could Secondary Flows Have Made Possible the Cross-Straight Transport and Explosive Invasion of *Rugulopteryx okamurae* Algae in the Strait of Gibraltar? *PLoS ONE* **2023**, *18*, e0285470. [[CrossRef](#)] [[PubMed](#)]
71. Bolado-Penagos, M.; González, C.J.; Chioua, J.; Sala, I.; Jesús Gomiz-Pascual, J.; Vázquez, Á.; Bruno, M. Submesoscale Processes in the Coastal Margins of the Strait of Gibraltar. The Trafalgar—Alboran Connection. *Prog. Oceanogr.* **2020**, *181*, 102219. [[CrossRef](#)]
72. Bruno, M.; Chioua, J.; Romero, J.; Vázquez, A.; Macías, D.; Dastis, C.; Ramírez-Romero, E.; Echevarría, F.; Reyes, J.; García, C.M. The Importance of Sub-Mesoscale Processes for the Exchange of Properties through the Strait of Gibraltar. *Prog. Oceanogr.* **2013**, *116*, 66–79. [[CrossRef](#)]
73. Haro, S.; Jimenez-Reina, J.; Bermejo, R.; Morrison, L. SoftwareX BioIntertidal Mapper Software: A Satellite Approach for NDVI-Based Intertidal Habitat Mapping. *SoftwareX* **2023**, *24*, 101520. [[CrossRef](#)]
74. Bayındır, C.; Namli, B. Efficient Sensing of von Kármán Vortices Using Compressive Sensing. *Comput. Fluids* **2021**, *226*, 104975. [[CrossRef](#)]
75. Bai, L.-H.; Xu, H. Accurate Estimation of Tidal Level Using Bidirectional Long Short-Term Memory Recurrent Neural Network. *Ocean Eng.* **2021**, *235*, 108765. [[CrossRef](#)]

Disclaimer/Publisher's Note: The statements, opinions and data contained in all publications are solely those of the individual author(s) and contributor(s) and not of MDPI and/or the editor(s). MDPI and/or the editor(s) disclaim responsibility for any injury to people or property resulting from any ideas, methods, instructions or products referred to in the content.